ISSN No. 2321-2705 | DOI: 10.51244/IJRSI |Volume XI Issue XI November 2024

Electrosynthesis and Characterization of Silver Selenide (Ag_2Se) and Cerium Doped Silver Selenide (Ce: Ag_2Se), Thin Films for Structural Properties Investigation

***Lois Ugomma Okafor, Donald Okoli, Azubike Josiah Ekpunobi**

Department of Physics and industrial physics, Nnamdi Azikiwe University, Awka Anambra State, Nigeria

***Corresponding Author**

DOI: https://doi.org/10.51244/IJRSI.2024.11110042

Received: 03 November 2024; Accepted: 12 November 2024; Published: 09 December 2024

ABSTRACT

In this research, Silver Selenide (Ag_2Se) and Cerium doped Silver Selenide (Ce: Ag_2Se), thin films have been successfully deposited onto FTO glass substrate using electrodeposition method. AgNO3 and Selenium powder were the precursors used for sources of Ag and Se ions respectively. Prototype of the films were again made and subjected to annealing at temperature of 150°C for 5 minutes to remove the element of moisture content in the deposited films. The Structural properties of Ag_2S and Ce doped Ag_2S thin films investigated using X-ray diffractometry. Variation of structural properties with concentration of cerium dopant**,** variation of structural properties with deposition time and variation of structural properties with pH were considered in this paper. The structural analysis of pure Ag_2Se and cerium-doped Ag_2Se thin films reveals significant changes in crystallographic properties with increasing cerium concentration. Ce-doped silver selenide thin films deposited at varying times of 15, 45, and 75 seconds correspond to the orthorhombic structural phase of Ag_2Se with the mineral name Naumannite, identified with the JCPDS file number 00-024-1041. Also Ce-doped silver selenide thin films deposited at different pH values of 4.1, 3.4, and 3.1 exhibit significant improvements in crystallographic properties

Key Words: Silver-Selenide, Structural properties, Electrodeposition, X– ray diffractometer machine

INTRODUCTION

Silver selenide (AgSe) is a superionic conductor that belongs to the group I–VI semiconductor materials [1], and it has an orthorhombic structure at low temperatures and changes to a cubic structure at 400 °C according to the corresponding report [2]. To synthesize the silver selenide thin films, many preparation techniques are available, such as the chemical vapor deposition, the adsorption process, the electrodeposition technique, the flash evaporation method, the solvo-thermal method, the vacuum evaporation process, and the explosive vaporization technique [2], [3], [4], [5], [6], [7], [8].

In literature, the properties of the films such as optical, structural and compositional have been investigated using UV-VIS Spectrophotometry, X-ray diffractometry and Rutherford backscattering Spectroscopy (RBS) analysis respectively to determine the possible areas of applications of the films. To the best of my knowledge, the reports on the structural properties of Ag_2Se and its thin films are incomplete. This present study presents Electrosynthesis and Characterization of Silver Selenide (Ag_2Se) and Cerium doped Silver Selenide (Ce: Ag_2Se), thin films for structural properties investigation. Variation of structural properties with concentration of cerium dopant**,** variation of structural properties with deposition time and variation of structural properties with pH were investigated in this paper.

Experimental Detail

The Silver Selenide (Ag_2Se) and Cerium doped Silver Selenide (Ce: Ag_2Se), thin films were deposited on FTO

ISSN No. 2321-2705 | DOI: 10.51244/IJRSI |Volume XI Issue XI November 2024

glass substrate using electrodeposition technique. The films were synthesized from silver trioxonitrate (v) (AgNO3) and selenium (Se) powder as sources of Ag and Se. We adopted a three-electrode configuration for depositing thin films onto conducting substrates. The conducting substrate, specifically FTO, was used as the cathode or working electrode. A platinum electrode functioned as the anode or counter electrode, while a silver/silver chloride (Ag/AgCl) electrode served as the reference electrode. The energy supply for the electrodeposition setup is provided by a Dazheng digital DC-power supply unit, specifically the PS-1502A model. Two digital multimeters, the DT9201A CE and the highly sensitive Mastech: MY60 were employed for measuring voltage and current, respectively. The Mastech: MY60 multimeter is capable of measuring currents within the range of 10^{-6} A. The FTO glass substrates were subjected to pre-treatment by cleaning with detergent, acetone, distilled water and dry in oven at 100 ^{0}C for 10 minutes and allowed to cool in air before use

Preparation of Precursors

Silver trioxonitrate(V)

Silver trioxonitrate (V) is an inorganic compound with chemical formula $AgNO_3$. It is a versatile precursor to many other silver compounds. It is a colorless salt with molar mass of 169.87 g/mol. About 256 g of the salt is soluble in 100 mL at 25 °C. In this work, silver trioxonitrate (V) served as precursor for Ag ion and various concentrations (0.10 M and 0.01 M) of silver trioxonitrate (V) was prepared by dissolving particular amount of the compound in 100 ml of distilled water. The calculations of the reacting mass (R.M) used were given below.

$$\text{R. M.} = \frac{0.10\times169.87\times100}{1000} = 1.70\ g \qquad 1$$

$$\text{R. M.} = \frac{0.01\times169.87\times100}{1000} = 0.17\ g \qquad 2$$

Selenium (IV) oxide

SeO_2 has a molecular weight of 110.96 g and it is soluble in water, about 39.5 g can dissolve in 100 ml of water at room temperature. Selenium (IV) oxide served as precursor for selenium ion. In this work, 0.20 mole solution of SeO_2 was prepared by dissolving 5.55 g in 250 ml of distilled water.

$$RM = \frac{0.20\times110.96\times250}{1000} = 5.55\ g \qquad 3$$

Electrodeposition of thin films

We adopted a three-electrode configuration for depositing thin films onto conducting substrates. The conducting substrate, specifically FTO, was used as the cathode or working electrode. A platinum electrode functioned as the anode or counter electrode, while a silver/silver chloride (Ag/AgCl) electrode served as the reference electrode. The energy supply for the electrodeposition setup is provided by a Dazheng digital DC-power supply unit, specifically the PS-1502A model. Two digital multimeters, the DT9201A CE and the highly sensitive Mastech: MY60 were employed for measuring voltage and current, respectively. The Mastech: MY60 multimeter is capable of measuring currents within the range of 10^{-6} A.

Electrodeposition of silver selenide and cerium doped silver selenide ($Ce:AgSe$) thin films

For electrodeposition of silver selenide thin film on FTO substrate, aqueous electrolytic bath composed of 20 ml of 0.10 M of silver trioxonitrate (V) and 5 ml of 1.0 M of H_2SO_4were poured into the electrolytic bath. The mixture was stirred for 5 minutes. This was followed by addition of 15 ml of 0.1 M of selenium (IV) oxide solution to the mixture. This followed with another stirring for 5 minutes. After stirring, the three electrodes were immersed into the bath containing the electrolytic solution and 2 volts was allowed to pass through the setup for 30 seconds. After the allowed time, dark film of Ag_2Se was found to be deposited on the conductive surface of the FTO substrate. The deposited Ag_2Se thin film was heat-treated at 100 ℃ for 10 minute to

ISSN No. 2321-2705 | DOI: 10.51244/IJRSI |Volume XI Issue XI November 2024

remove water and increase the crystallinity of the deposited thin films. The mechanism of the formation of silver selenide and cerium doped silver selenide is shown in equation (4) and (5).

$$2Ag^{+} + Se^{4+} + 2e^{-} \longrightarrow Ag_2Se \quad 4$$

$$2Ag^{+} + Se^{4+} + Ce^{4+} + 2e^{-} \longrightarrow Ce{:}Ag_2Se \quad 5$$

Optimization of Ce ion concentration for Ce: Ag_2Sethin films

For the deposition of Ce doped Ag_2Se thin films, 0.05 M of cerium (IV) tetraoxosulphatetetrahydrate was used. Similar procedure used for deposition of silver selenide thin film was adopted but with addition of different volume concentrations of 0.05 M of cerium (IV) tetraoxosulphatetetrahydrate as shown in Table 1. Four samples with different dopant volume concentrations of 1 ml, 2 ml, 3 ml and 4 ml were fabricated.

Table 1: Bath parameter for deposition of Ag_2Se and Ce doped Ag_2Se thin films

0.10 M of $AgNO_3$	**0.10 M of SeO_2**	**0.05 M of $CeSO_4{\cdot}4H_2O$**	**1.0 M of H_2SO_4**	**Applied Voltage**	**Time**
Vol. (ml)	Vol. (ml)	Vol. (ml)	Vol. (ml)	(volts)	(sec.)
20.00	15.00	-	5.00	2.00	30
20.00	15.00	1.00	5.00	2.00	30
20.00	15.00	2.00	5.00	2.00	30
20.00	15.00	3.00	5.00	2.00	30
20.00	15.00	4.00	5.00	2.00	30

Optimization of deposition time for $Ce{:}Ag_2Se$ thin films

For time optimization of Ce doped Ag_2Se thin films, similar procedure used for deposition of cerium doped silver selenide thin film was adopted. 0.10 M of silver trioxonitrate (V), 1.0 M of H_2SO_4, 0.1 M of selenium (IV) oxide and 0.05 M of cerium (IV) tetraoxosul phatetetrahydrate were used to deposit the desired thin film. Five films were deposited at time interval of 15 seconds, 30seconds, 45 seconds, 60 seconds and 75 seconds. Table 2 shows the constituent of the electrolytic baths used for the deposition of Ce doped Ag_2Se at varying deposition time.

Table 2: Bath parameter for time optimized Ce: Ag_2Se thin films

0.10 M of $AgNO_3$	**0.10 M of SeO_2**	**0.05 M of $CeSO_4{\cdot}4H_2O$**	**1.0 M of H_2SO_4**	**Applied Voltage**	**Time**
Vol. (ml)	Vol. (ml)	Vol. (ml)	Vol. (ml)	(volts)	(sec.)
20.00	15.00	2.00	5.00	2.00	15
20.00	15.00	2..00	5.00	2.00	30
20.00	15.00	2.00	5.00	2.00	45
20.00	15.00	2..00	5.00	2.00	60
20.00	15.00	2.00	5.00	2.00	75

ISSN No. 2321-2705 | DOI: 10.51244/IJRSI |Volume XI Issue XI November 2024

Optimization of deposition pH for Ce: Ag_2Se thin films

For pH optimization of Ce doped Ag_2Se thin films, similar procedures used for deposition of cerium doped silver selenide thin film were maintained. The 0.10 M of silver trioxonitrate (V), 1.0 M of H_2SO_4, 0.10 M of selenium (IV) oxide and 0.05 M of cerium (IV) tetraoxosul phatetetrahydrate were used for the deposition of Ce doped Ag_2Se thin films at varying pH. Five films were deposited with different volume concentration of H_2SO_4. 1 ml. 2 ml, 3 ml, 4 ml and 5 ml of H_2SO_4 were used to achieve variation in pH of the medium. Table 3 shows the constituent of the electrolytic baths used for the deposition of Ce doped Ag_2Se at varying pH.

Table 3: Bath parameter for pH optimized Ce: Ag_2Se thin films

0.10 M of $AgNO_3$	**0.10 M of SeO_2**	**0.05 M of $CeSO_4 \cdot 4H_2O$**	**1.0 M of H_2SO_4**	**Applied Voltage**	**Time**
Vol. (ml)	Vol. (ml)	Vol. (ml)	Vol. (ml)	(volts)	(sec.)
20.00	15.00	2.00	1.00	2.00	30
20.00	15.00	2..00	2.00	2.00	30
20.00	15.00	2.00	3.00	2.00	30
20.00	15.00	2..00	4.00	2.00	30
20.00	15.00	2.00	5.00	2.00	30

RESULTS AND DISCUSSION

Variation of structural properties with concentration of cerium dopant

The structural analysis of pure Ag_2Se and cerium-doped Ag_2Se thin films, as detailed in Table 4 and illustrated in Figure 1, reveals significant changes in crystallographic properties with increasing cerium concentration. Pure Ag_2Se, identified with the JCPDS file number 00-024-1041 and the mineral name Naumannite in its orthorhombic structural phase, exhibits diffraction peaks corresponding to the (112), (031), and (201) planes at 2θ angles of 33.827°, 39.996°, and 43.422°, respectively. Average crystallite size of pure Ag_2Se thin films was found to be 29.493 nm withmicro-strain of 1.167×10^{-3} and dislocation density of 3.745×10^{-3} lines/nm².

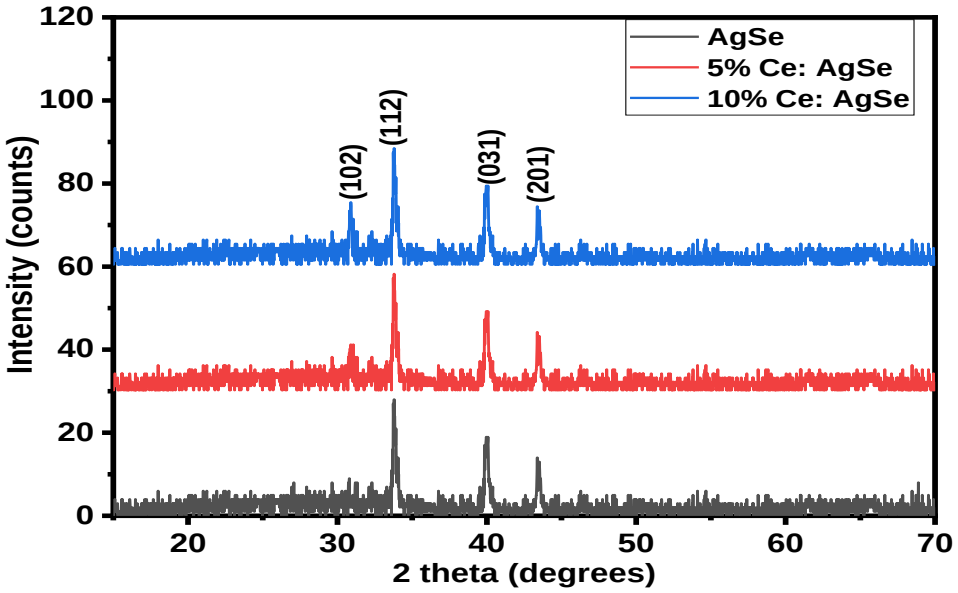

Figure 1: Diffractogram of Ag_2Se and cerium doped Ag_2Se deposited with different percentage concentration of dopant

ISSN No. 2321-2705 | DOI: 10.51244/IJRSI |Volume XI Issue XI November 2024

Table 4: Structural parameters of Ag_2Se and cerium doped Ag_2Se thin films

Doping Level	**2 Theta (°)**	**hkl**	**FWHM (°)**	**Crystallite Size (nm)**	**Micro-strain (ε) × 10^{-3}**	**Dislocation Density × 10^{-3} $lines/nm^2$**
Ag_2Se	33.827	112	0.307	28.287	4.399	1.250
	39.996	031	0.319	27.673	3.825	1.306
	43.422	201	0.275	32.520	3.010	0.946
			Average	**29.493**	**1.167**	**3.745**
5% Ce:Ag_2Se	30.900	102	0.207	41.496	0.581	3.275
	33.827	112	0.369	23.528	1.806	5.289
	39.896	031	0.320	27.589	1.314	3.846
	43.382	201	0.276	32.380	0.954	3.025
			Average	**31.248**	**1.164**	**3.859**
10% Ce:Ag_2Se	30.888	102	0.217	39.751	0.633	3.420
	33.827	112	0.307	28.230	1.255	4.408
	39.996	031	0.320	27.619	1.311	3.833
	43.472	201	0.235	37.936	0.695	2.577
			Average	**33.384**	**0.973**	**3.560**

Upon doping with 5% cerium, peaks appear at 30.900°, 33.827°, 39.896°, and 43.382° corresponding to the (102), (112), (031), and (201) planes, respectively. The FWHM values remain consistent, indicating no peak broadening and suggesting an increase in crystallinity. The average crystallite size increases to 31.248 nm, micro-strain slightly decreases to 1.164 × 10^{-3}, and dislocation density averages around 3.859 × 10^{-3} lines/nm². Notably, the intensity of the peaks increases, suggesting enhanced crystallinity with cerium doping.

Further doping to 10% cerium shows similar trends, with peak positions at 30.888°, 33.827°, 39.996°, and 43.472° and a further increase in average crystallite size to 33.384 nm, reduction in micro-strain to 0.973 × 10^{-3}, and dislocation density of 3.560 × 10^{-3} lines/nm². Figure 4.4 illustrates these observations, where the intensity of the diffraction peaks increases with higher cerium concentration, indicating improved crystallinity. These findings suggest that cerium doping promotes grain growth, reduces lattice distortions, and enhances crystallinity, thereby tailoring the material's properties for potential applications.

Variation of structural properties with deposition time

Figure 2 shows the diffractogram of Ce doped silver selenide thin films deposited at different time. Ce-doped silver selenide thin films deposited at varying times of 15, 45, and 75 seconds correspond to the orthorhombic structural phase of Ag_2Se with the mineral name Naumannite, identified with the JCPDS file number 00-024-1041. The structural analysis presented in Table 5 and illustrated in Figure 2 reveals significant improvements in crystallographic properties with increasing deposition times. For films deposited at 15 seconds, no distinct peaks are observed, indicating very low crystallinity or an amorphous structure. In contrast, films deposited at 45 seconds exhibit distinct peaks corresponding to the (112), (031), and (201) planes, with crystallite sizes ranging from 28.489 nm to 34.116 nm, dislocation densities ranging from 0.859 × 10^{-3} to 1.232 × 10^{-3} lines/nm², and lattice strains ranging from 2.865 × 10^{-3} to 4.311 × 10^{-3}, with average values of 30.489 nm, 1.097 × 10^{-3} lines/nm², and 3.631 × 10^{-3}, respectively.

ISSN No. 2321-2705 | DOI: 10.51244/IJRSI |Volume XI Issue XI November 2024

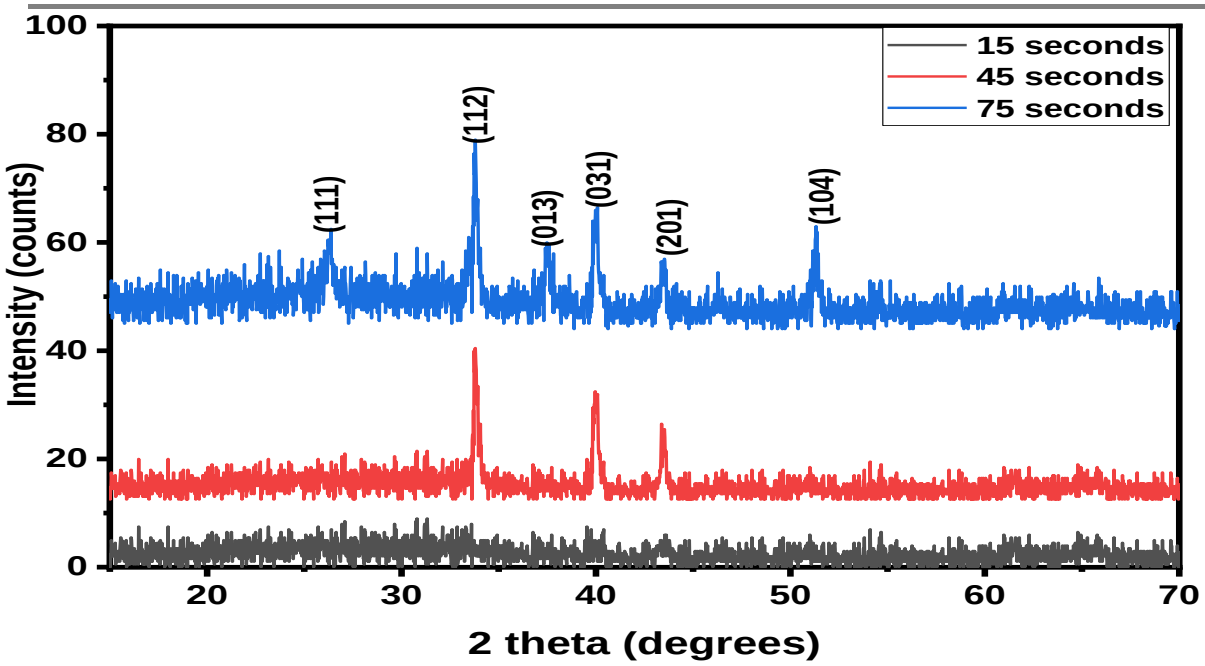

Figure 2: Diffractogram of cerium doped Ag_2Se deposited under different deposition time

Table 5: Structural parameters of cerium doped Ag_2Se thin films deposited at different time

Deposition Time	2 Theta (°)	hkl	FWHM (°)	Crystallite Size (nm)	Dislocation Density $\times 10^{-3}$ $lines/nm^2$	Micro-strain (ε) $\times 10^{-3}$
45 seconds	33.826	112	0.300	28.864	1.200	4.311
	39.997	031	0.310	28.489	1.232	3.716
	43.474	201	0.262	34.116	0.859	2.865
			Average	**30.489**	**1.097**	**3.631**
75 seconds	28.214	111	0.225	38.005	0.692	3.908
	33.802	112	0.350	24.750	1.632	5.032
	37.518	013	0.347	25.242	1.569	4.460
	39.996	031	0.324	27.281	1.344	3.880
	43.512	201	0.152	58.871	0.289	1.659
	51.312	104	0.338	27.233	1.348	3.070
			Average	**33.564**	**1.146**	**3.668**

For films deposited for 75 seconds, additional peaks at (111), (013), and (104) planes are observed, with crystallite sizes ranging from 24.750 nm to 58.871 nm, dislocation densities ranging from 0.289 × 10^{-3} to 1.632 × 10^{-3} lines/nm², and lattice strains ranging from 1.659 × 10^{-3} to 5.032 × 10^{-3}, with average values of 33.564 nm, 1.146 × 10^{-3} lines/nm², and 3.668 × 10^{-3}, respectively. The intensity of these peaks increases with longer deposition times, suggesting enhanced crystal growth. Overall, the data from Table 4.5 and Figure 4.5 confirm that longer deposition times promote grain growth, reduce lattice distortions, and enhance crystallinity, thereby improving the material's properties for potential applications

ISSN No. 2321-2705 | DOI: 10.51244/IJRSI |Volume XI Issue XI November 2024

Variation of structural properties with pH

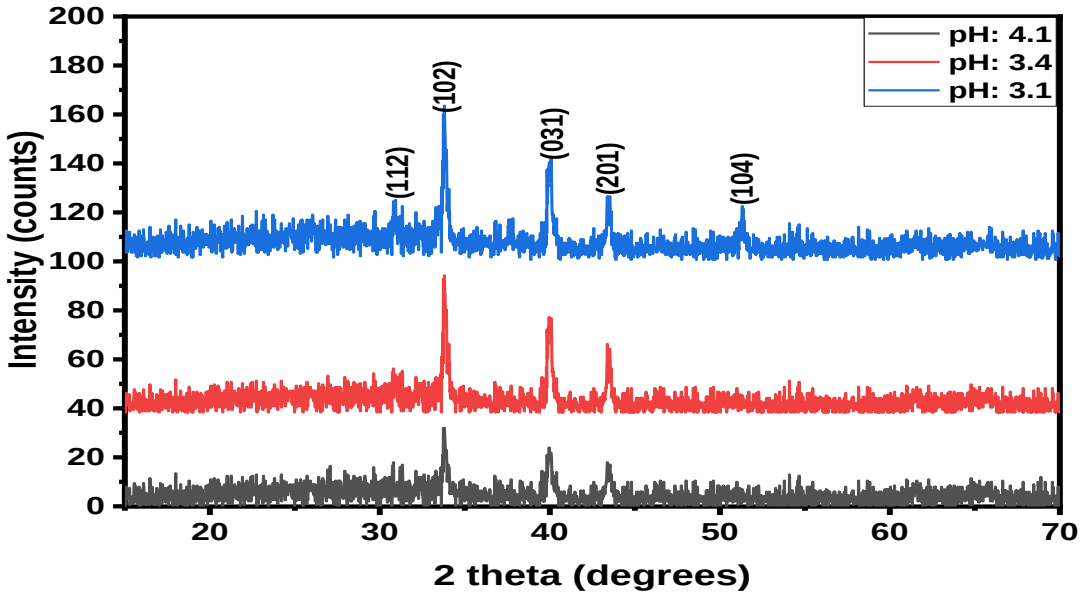

Figure 3: Diffractogram of cerium doped Ag_2Se thin films deposited at different pH of 4.1, 3.4 and 3.1.

Figure 3 shows the diffractogram of Ce doped silver selenide thin films deposited at different pH. Ce-doped silver selenide thin films deposited at different pH values of 4.1, 3.4, and 3.1 exhibit significant improvements in crystallographic properties, as detailed in Table 6 and illustrated in Figure 3. The structural analysis reveals that films deposited at pH 4.1 show distinct peaks corresponding to the (102), (031), and (201) planes, with crystallite sizes ranging from 25.473 nm to 29.620 nm, dislocation density from $1.140 \times 10^{-3} line/nm^2$ to $1.541 \times 10^{-3} line/nm^2$, and micro-strain from 3.839×10^{-3} to 4.202×10^{-3}, with average values of 26.948 nm, $1.396 \times 10^{-3} line/nm^2$, and 4.051×10^{-3}respectively. As the pH decreases to 3.4, the films exhibit peaks at (112), (102), (031), and (201) planes, with crystallite sizes ranging from 28.210 nm to 42.664 nm, dislocation density from $0.549 \times 10^{-3} line/nm^2$ to $1.257 \times 10^{-3} line/nm^2$, and micro-strain from 2.293×10^{-3} to 4.497×10^{-3}, with average values of 29.039 nm, $1.189 \times 10^{-3} line/nm^2$, and 4.195×10^{-3} respectively.

Table 6: Structural parameters of cerium doped Ag_2Se thin films deposited at different pH

pH	**2 Theta (°)**	**hkl**	**FWHM (°)**	**Crystallite Size (nm)**	**Dislocation Density $\times 10^{-3}$ $lines/nm^2$**	**Micro-strain (ε) $\times 10^{-3}$**
4.1	33.821	102	0.293	29.620	1.140	4.202
	39.994	031	0.343	25.751	1.508	4.111
	43.463	201	0.351	25.473	1.541	3.839
			Average	**26.948**	**1.396**	**4.051**
3.4	30.927	112	0.285	30.195	1.097	4.497
	33.827	102	0.302	28.713	1.213	4.334
	39.996	031	0.313	28.210	1.257	3.753
	43.450	201	0.209	42.664	0.549	2.293
			Average	**29.039**	**1.189**	**4.195**
3.1	29.894	112	0.244	35.259	0.804	3.981

ISSN No. 2321-2705 | DOI: 10.51244/IJRSI |Volume XI Issue XI November 2024

	33.815	102	0.296	29.278	1.167	4.252
	39.996	031	0.320	27.560	1.317	3.841
	43.470	201	0.307	29.104	1.181	3.359
	51.317	104	0.307	29.993	1.112	2.788
			Average	**30.300**	**1.117**	**3.858**

At pH 3.1, additional peaks at (112), (102), (031), (201), and (104) planes are observed, with crystallite sizes ranging from 27.560 nm to 35.259 nm, dislocation density from $0.804 \times 10^{-3} line/nm^2$ to $1.317 \times 10^{-3} line/nm^2$ and dislocation density from 2.788×10^{-3} to 4.252×10^{-3} with average values of 30.300 nm, $1.117 \times 10^{-3} line/nm^2$, and 3.858×10^{-3} respectively. The intensity of the peaks increases with lower pH levels, indicating enhanced crystallinity. The reduction in micro-strain and dislocation density suggests fewer defects and reduced lattice distortions. Overall, the data from Table 6 and Figure 3 confirm that lower pH levels during deposition promote grain growth, enhance crystallinity, and improve the material properties of Ce-doped Ag_2Se thin films for potential applications.

CONCLUSION

In this research, Ag_2S and Ce doped Ag_2S thin film were successfully synthesized and characterized for structural properties analysis. Variations of structural properties with percentage concentration of cerium dopant, with deposition time and with concentration of pH were considered in this work.

ACKNOWLEDGEMENT

The authors appreciate the efforts of the team of scientists and technologists at Nano Research Laboratory, University of Nigeria Nsukka, Enugu State Nigeria

Conflict of Interest

The authors declared that there is no conflict of interest in the course of this research work.

REFERENCES

1. Chukwudi Benjamin MUOMELIRI, Ngozi Agatha OKEREKE, Augustine Nwode NWORI, Uchechukwu Vincent OKPALA and Nonso Livinus OKOLI (2024), Electrosynthesis and Characterizations of Aluminum Silver Selenide ($Alagse_2$), Thin Films for Possible Device Applications, INTERNATIONAL JOURNAL OF RESEARCH AND SCIENTIFIC INNOVATION (IJRSI), Volume XI, Issue IX
2. Khanna P.K., and Das B.K. (2004), Novel synthesis of silver selenide nano-powder from silver nitrate and organo-selenium compound, Materials Letters, Volume 58, Issue 6, Pages 1030-1034
3. Subhash Chander and M.S. Dhaka (2016), Impact of thermal annealing on physical properties of vacuum evaporated polycrystalline CdTe thin films for solar cell applications, Physica E: Low-dimensional Systems and Nanostructures Volume 80, Pages 62-68
4. Ammar Qasem , Shoroog Alraddadi , Eshraq Al-Amery , H.A. Alrafai , E.R. Shaaban (2023), Remarkable effects of laser irradiation in adjusting the structural, morphological, and optical properties of spray pyrolysis-synthesized NiO nanostructured films for optoelectronic applications. Optics & Laser Technology Volume 164, 109488
5. Adel Madani, Manar Alghamdi, Bedour Alamri, Shoaa Althobaiti (2023), Structural and optical properties of Sb–$BaTiO_3$ and Y– $BaTiO_3$ doped ceramics prepared by solid-state reaction, Optical Materials, Volume 137, March 2023, 113480
6. Ahmed M. El-Mahalawy , S.A. Mansour , Ahmed R. Wassel , Asmaa E. Mohamed , Shehab E. Ali (2022), Impact of structural and optical properties tunability of $SnSe_2$ thin films on its optoelectronic

ISSN No. 2321-2705 | DOI: 10.51244/IJRSI |Volume XI Issue XI November 2024

properties, Surfaces and Interfaces, Volume 33, October 2022, 10225

7. Faisal G. AL-Maqate , Ammar Qasem , Thamer Alomayri , Adel Madani (2022), Profundity study on structural and optical properties of heavy oil fly ash (HOFA) doped calcium carbonate ($CaCO_3$) nanostructures and thin films for optoelectronic applications, Optical Materials, Volume 131,
8. Hosam M. Gomaa and I. S. Yahia (2022), toward a novel and accurate relationship between electrical and optical conductivity in opto-material sciences: New strategy, Journal of Computational Electronics, Volume 21, pages 1396–1403